MONITORING OF AN HYDRAULIC STRUCTURE AFFECTED BY ASR: A CASE STUDY

Patrice Rivard*, Gérard Ballivy, Clermont Gravel, Francois Saint-Pierre

Department of Civil Engineering, Université de Sherbrooke
SHERBROOKE, J1K 2R1, Canada

Abstract

Relevant and effective instruments and techniques must be selected for monitoring hydraulic structures affected by Alkali-Silica Reaction ("ASR"). A program aiming at assessing the condition of an hydraulic structure affected by ASR is presented here. The structure has been exhibiting signs of ASR for more than 30 years and shows various levels of damage.

The program encompassed different components, consisting: (1) stress measurement, (2) evaluation of concrete condition by nondestructive methods without drilling (seismic tomography), (3) the evaluation of the mechanical, physical and petrographic properties of the concrete determined from cores recovered from full-length boreholes.

The results of this case study suggest that ASR may generate relatively little damage in structures and that the concrete mechanical properties do not seem to be significantly affected despite high expansion levels measured in this structure. A major crack was localized with the seismic tomography. The monitoring program will be used to follow the development of ASR in the structure.

Keywords: damage, mechanical properties, nondestructive testing, petrography, management, tomography

1 INTRODUCTION

Like some other deterioration mechanisms that affect concrete, alkali-silica reaction is progressive, variable and not easy to predict. Thus, the management of hydraulic structures affected by ASR requires a systematic assessment of the state of the reaction. Nevertheless, in most cases documented thus far, only a limited range of investigation methods has been used, and their effectiveness has not always been conclusive. For example, visual inspection can lead to a global evaluation of the extent of ASR damage but it remains a surface investigation that is primarily qualitative, and it mainly depends on the experience and skills of the investigator.

In addition, it is known that the effect of ASR on the mechanical properties of the concrete varies, and that ASR does not develop homogeneously in the affected structure [1]. Regarding the mechanical properties, the compressive strength does not seem to be a suitable criterion for ASR assessment, whereas the static Young modulus and the tensile strength are more sensitive, at least on concrete made in the laboratory [2,3]. Regarding nondestructive techniques ("ND"), only few of these methods have been applied to ASR, and have mainly consisted of measuring ultrasonic velocity in laboratory [2,3,4]. Very little information exists regarding ND methods applied to field cases.

In the context where limited funds are generally allowed for monitoring hydraulic structures affected by ASR, relevant and effective instruments and techniques must be selected. This paper presents a large program that was designed to assess the extent and distribution of damage associated with ASR in a large hydraulic structure located in Eastern Canada.

2 INVESTIGATED SITE

The study was carried out on a large hydraulic structure located in Eastern Canada. It was built nearly 50 years ago and is affected by ASR to various degrees, detected approximately 20 years after its construction. The ASR in this structure is due to the use of a reactive crushed siliceous limestone as coarse aggregate in the concrete. Several recurring operating problems have been reported over the last years. Horizontal displacements related to the expansion of concrete vary between 0.1 mm/year and 1.6 mm/year.

* Correspondence to: patrice.rivard@usherbrooke.ca

3 MONITORING PROGRAM

3.1 Stress measurements

The stresses in the concrete body were estimated using a technique that enables the direct measurement of in-situ concrete stress, based on strain relief. The strain field is relieved by slot cutting the material; the strain change in the relieved area can be measured. Usually, the stress is calculated taking into account the elastic properties of the material and the geometry of the cut; however the modulus of elasticity varies with concrete mix, age, curing and environmental conditions. In order to eliminate the need to know the elastic properties of the concrete, the procedure requires a flat jack that is inserted into the slot and pressurized. As a result, the initial strain field will be restored. The combination of the measured data on strain and pressure provides the value of the stress.

Measurements were carried out in groups of three inside a gallery, on the walls and on the floor. Such grouping of three measurements allows defining the three main stresses (σx, σy, σz). Two zones were subjected to stress measurements. The results indicated that stresses in transverse axis were virtually nil (mean of 0.1 MPa). This value was expected since the expansion is not restrained along this axis. Compressive stresses of 2.0 and 3.5 MPa were measured along the longitudinal axis, which is typical of stress generated by ASR in hydraulic structures [5]. The stresses measured on the vertical axis yielded both compression and tensile stresses. In one case, a compressive stress of 1.3 MPa was measured. In another case, a tensile stress of 0.2 MPa was measured. This tensile stress was not expected because of the load resulting from the concrete above the measurement point. However, this measurement was carried out near a room. It may be inferred that this room disturbs the surrounding stress field. This result points out the importance regarding the appropriate selection of the site of measurements.

3.2 Seismic Tomography

Procedure

Seismic tomography enables the mapping of sections in order to "see" the distribution of the concrete quality in 2D. The different zones visible on the investigated sections correspond to the variations in the propagation velocity of compression waves through the concrete. These waves, generated by a mechanical impact, are the first waves to be recorded by the receiver, so they are also called primary waves or *P*-waves. The variations of velocity are mainly related to the mechanical properties of the concrete, as well as the presence of large defect such as cracks or voids. The aim of a tomography is thus to identify problematic areas in a concrete section. For instance, seismic tomography can help in determining the type of intervention to be carried out on the structure by targeting zones of different quality. Further, relevant information on tomography can be found in specialized papers [6,7].

The configurations used for data acquisition are shown in Figure 1. Each straight line represents the supposed path followed by *P*-waves between the impact and the receiver. Eight tomographies were performed. These configurations enabled coverage of about 60% of the section. The left part of the structure was not accessible due to the presence of backfill. This zone was investigated from the culvert with an alternative method using surface waves (Rayleigh waves) and will not be presented in this paper. This method, called FK method, has been recently optimized for the needs of civil infrastructure and results have been previously published [8].

The impacts for generating *P*-waves were done with hammers of various gauges: 225 g, 450 g, 680 g, 1.8 kg, 3.6 kg and 4.5 kg. Heavier hammers were used to generate a sufficient amount of energy, as well as to improve the recording of the *P*-wave arrival time, when the covered distances were too long (e.g., where the maximum distance was about 12 m).

In order to ensure good reproducibility of measurements, the signals of at least two hammer impacts were recorded for each measurement point. A 0.5 m spacing grid was used between each position (both impact and receiver). The signal acquisition was performed with *Microsis* system. This system enables acquiring and visualizing simultaneously, and in real time, 12 signals with a resolution of 12 bits. Nearly 600 signals were measured to obtain the precision required for the calculation of wave velocities. The tomography was carried out with *3DTOM* to obtain the velocity mapping.

Results

The velocities calculated from the inversion vary approximately between 2000 and 4500 m/s (Figure 3). Since the variations are significant, low velocities are assumed to be caused by cracks in the concrete, rather than by a reduction in the modulus of elasticity. Although it could be difficult to set limits regarding the concrete condition, it is suggested that a velocity above 3000 m/s is indicative of a good quality concrete, which is in accordance with the ASTM C 597.

Two areas of low velocities were identified. The first area, which is the most critical, was located between the gallery and the surface, and gave velocities around 2200 m/s. This low-velocity zone (red in Fig. 2) is caused by a tensile crack that is partially visible in the gallery. The tomography indicated that the crack would virtually extend from the gallery to the surface.

An area with various low-velocity zones was found between the lower corner of gallery and the culvert below. Velocities varied between 2000 and 3000 m/s. Both distress zones were mainly located in the axis connecting the corners of the galleries. This would result from the expansion of concrete caused by the ASR. The swelling of the concrete itself did not create major cracking; this occurs at location where stresses are concentrated, such as at corners of the galleries. In this case, the deformation of the structure toward the left induced tensile stress in the areas depicted in red on the tomography (Fig. 2) and consequently, cracks have been created. This is in accordance with the stress values that were measured in the gallery.

3.3 Mechanical properties (on drilled cores)

Cores of 80 mm in diameter were collected along two vertical boreholes (referred to as BH-3 and BH-5) that run through the structure, down to the bedrock located about 14 meters below surface. The cores were quickly stored in plastic tubes that were then sealed at both ends. The testing program began about two weeks after coring. The compressive strength, indirect tensile strength (splitting) and Young's modulus were determined on selected cores. Testing was performed in compliance with ASTM standards.

Compressive strength values varied from 19.7 to 45.2 MPa (Fig. 3). Average values were 28 MPa for BH-3 and 25 MPa for BH-5, which is quite normal for a mass concrete of more than 40 years' age. No specific trend was observed, although the samples located near the surface (first two meters) showed low compressive strength values. Concrete at the bottom of the boreholes (i.e. close to the bedrock interface) yielded relatively high compressive strength values.

Indirect tensile strength values ranged from 2.4 to 4.3 MPa (Fig. 4). Average values were 3.2 MPa for BH-3 and 3.3 MPa for BH-5. Samples from the near-surface zone of BH-5 also showed low tensile strength. No specific trend was observed.

The values of the static Young's modulus varied from 13.9 to 26.2 GPa (Fig. 5). Average values were 20.5 and 19.3 GPa for BH-3 and BH-5, respectively. Again, lowest values were obtained close to the surface while samples from the bottom of the borehole had high values.

These results suggest that ASR and climatic agents had a significant effect on the concrete condition near the surface, which agree with what is found in the literature [1]. The weakest mechanical properties were mainly obtained in concrete within the first two meters of the surface. Nevertheless, concrete condition remains good along the boreholes. The lower part of the structure did not seem to suffer from ASR, reaching quite high values, as an increasing trend could be observed from about 12 m deep.

3.4 Ultrasonic pulse velocity (on drilled cores)

The velocity of compression (*P*) and shear (*S*) waves traveling through the concrete core was determined in accordance with the ASTM C597 standard. Compression and shear waves showed about the same trend (Fig. 6). The *P*-wave velocities varied from 3000 m/s to 5095 m/s, while *S*-wave velocities lied between 1660 m/s and 3440 m/s. In general, *P*-wave velocities higher than 3500 m/s are considered to be indicative of a good condition concrete.

Values showed a certain scattering. In BH-3, slow velocities (for both *P* and S waves) were found close to the surface, and an increasing trend was observed at the bottom (Fig. 6a). Surprisingly, high values were found close to the surface of BH-5. Like in BH-3, values increase with depth below about 12 m. The *S*-waves did not appear to be more sensitive to ASR than *P*-waves.

3.5 Petrographic examination

The damage to concrete was also assessed by petrographic examination, conducted with the Damage Rating Index method [9,10]. The method, which is not a standard procedure and as conducted herein, consists of counting every typical feature associated with ASR (e.g. dark rim around aggregate particle) on a polished section observed with a stereomicroscope at a magnification of 16x. A weighting factor is applied specifically to each petrographic feature. The result is a numeric value providing a measure of damage in the concrete due primarily to ASR. However, other causes of concrete deterioration, e.g. frost action, may also contribute to the index.

Petrographic examination confirmed that the concrete is affected, at various levels, by ASR. Several features associated with ASR were observed, such as cracks filled with gel, cracks passing

through aggregates and through cement paste, etc. (Fig. 7). The *Damage Rating Index* (DRI) calculated from the cores ranged from 160 to 480, which is quite high according to the authors' experience. Although no accepted limits have been adopted yet, DRI value above about 30 is considered by the authors as indicative of significant ASR in the concrete [9,10].

Detailed DRI results are provided in Table 1 and the DRI values with depth are shown in Figure 8. The most deteriorated zones – as indicated by the DRI – correspond to the first meters from the surface. High DRI values were mainly due to the contribution of cracks in cement paste filled with gel, as well, as cracks with gel in coarse aggregates (Table 1). Cracks were relatively thin (opening < 1 mm). The number of cracks (filled or not with gel) generally decreases with depth. Only few reaction rims and debonded aggregates were observed.

It can be seen from Figure 8 that the less damaged concrete is found at the bottom, which is in accordance with mechanical and ND results.

4 CONCLUSION

In mass concrete structure, such as dams and locks, ASR is thought to mainly affect the surface concrete. This study showed that, despite obvious evidence of ASR (cracking, recurrent operating problems) and significant displacements observed on the structure, the concrete did not suffer from reduction of mechanical properties, except in the first two meters from the surface. This deterioration is closely associated with climatic agents, such as freeze/thaw cycles.

The stresses that were measured are in accordance with the observed damage and typical of stress induced by ASR in a large structure. The transverse stress is virtually nil, which is due to the more or less free unstrained expansion in this axis and the relief associated with the crack (found with the tomography). Higher compression stresses were measured in the confined longitudinal axis, where values were about 2-3 MPa.

The seismic tomography allowed adequate cover of the structure and enabled locating a major tensile crack in the gallery (and therefore estimating its depth). A second tomography would be carried out in about 5 years in an attempt to assess the evolution of this crack and the potential creation of new major cracks.

Regarding the methods that were used to assess damage on drilled cores, the following conclusions may be drawn:

- Mechanical properties were slightly affected in the zone two meters below the surface, and high scatter was observed in the data obtained from this study. The static Young's modulus appears to be the most relevant parameter to quantify ASR damage.
- *P*-waves and *S*-waves yielded about the same trend, so *S*-waves did not appear to be more sensitive to ASR than *P*-waves.
- Petrographic examination should always be conducted on cores since it yields reliable results. Authors point out that DRI is not a standard test procedure and may lead to variable results depending on the operator's experience and skill.

This program will allow the monitoring of the progression of ASR in the structure for the next decade. The priority zones for the repair work can then be targeted, as well as estimating the thickness of concrete to be potentially removed for surface repair. Since ASR is a relatively slow reaction, it is expected to carry out these monitoring investigations every 5 years. It is thought that a shorter period between the investigations would not bring any additional relevant information.

5 REFERENCES

[1] Fournier, B, Bérubé, MA (2000): Alkali-aggregate reaction in concrete: a review of basic concepts and engineering implications. Canadian Journal of Civil Engineering, (27): 167-191.

[2] Swamy, RN, Al-Asali, MM (1988): Engineering Properties of concrete affected by alkali-silica reaction. ACI Materials Journal (85): 367-374.

[3] Ahmed, T, Burley, E, Rigden, S, Abu-Tair, A (2002): The effect of alkali reaction on the mechanical properties of concrete. Construction and Building Materials (17): 123-144.

[4] Saint-Pierre, F, Rivard, P, Ballivy, G (2007): Measurement of alkali-silica reaction progression by ultrasonic waves attenuation. Cement and Concrete Research, (37): 948-956.

[5] Bois, AP (1995): Auscultation des ouvrages en rocher ou en béton à l'aide du cylindre instrumenté de l'Université de Sherbrooke, Ph.D. thesis (in French), Université de Sherbrooke, Canada, 382 p.

[6] Buyukozturk, O (1998): Imaging of concrete structures. NDT & E International (31): 233-243.

[7] Grandjean, G (2006): Imaging subsurface objects by seismic *P*-wave tomography: numerical and experimental validations. Near Surface Geophysics (4): 279-287

[8] Al Wardany, R, Ballivy, G, Gallias, JL, Saleh, K, Rhazi, J (2007): Assessment of concrete slab quality and layering by guided and surface wave testing. ACI Materials Journal (104): 268-275.
[9] Grattan-Bellew, PE (1995): Laboratory evaluation of alkali-silica reaction in concrete from Saunders Generating station. ACI Materials Journal (92): 126-134.
[10] Rivard, P, Ballivy, G (2005): Assessment of the expansion related to alkali-silica reaction by the Damage Rating Index method. Construction and Building Materials, (19): 83-90.

6 ACKNOWLEDGEMENTS

Funding has been provided by the Natural Sciences and Engineering Research Council of Canada (NSERC) and by the St. Lawrence Seaway. The contribution of D. Charbonneau, R. Al-Wardany, J. Champagne and A. Quere is also acknowledged.

TABLE 1. Detailed petrographic data. Each petrographic feature value is weighted and expressed for a 100cm²-equivalent area.

Depth (m)	CA	CA+G	D	R	CP	CP+G	AV	**Total**
0.5	6.8	167	12.5	1.0	123	70.8	13.5	**394**
0.5	5.4	163	5.4	0	100	111	16.1	**400**
2.0	2.4	133	8.6	0	119	42.3	9.1	**314**
2.3	7.1	119	7.8	1.3	132	77.9	11.0	**357**
3.1	4.2	195	0	0	157	118	16.5	**490**
3.9	3.7	85.4	0	2.6	104	37.5	2.6	**236**
4.3	5.5	92.8	2.8	0	94.7	22.7	7.6	**226**
8.3	9.4	129	0	0.48	98.1	53.9	8.2	**299**
8.9	2.0	155	2.7	2.7	71.4	78.6	11.2	**324**
9.6	6.0	102	2.9	0.48	73.1	7.69	6.3	**198**
9.8	5.0	179	0	1.6	91.7	54.2	8.3	**340**
11.3	4.1	121	2.6	0.4	39.7	20.7	8.2	**196**
12.8	4.1	87.5	3.8	0.6	95.0	25.0	3.1	**219**
13.8	2.2	90.0	0	0	55.0	10.0	2.5	**160**

Note. CA= crack in aggregate (factor: 0.5); CA+G = crack with gel in aggregate (factor: 2); D=aggregate debonded (factor: 3); R= reaction rim (factor: 0.5); CP= crack in cement paste (factor: 2); CA+G= crack with gel in cement paste (factor: 4); AV= gel in air void (factor: 0.5)

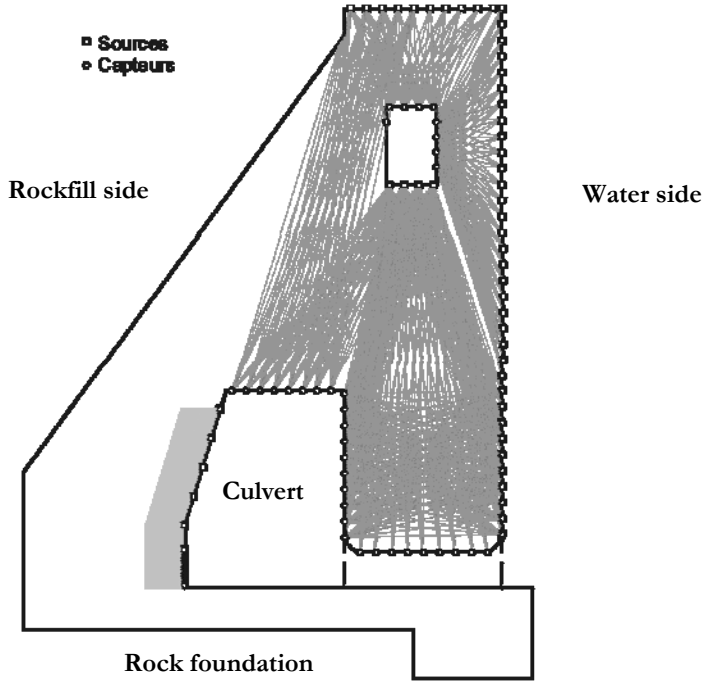

Figure 1: Cross-section of investigated structure showing configurations of impact-receiver for the tomographies. The shaded zone was covered with FK method.

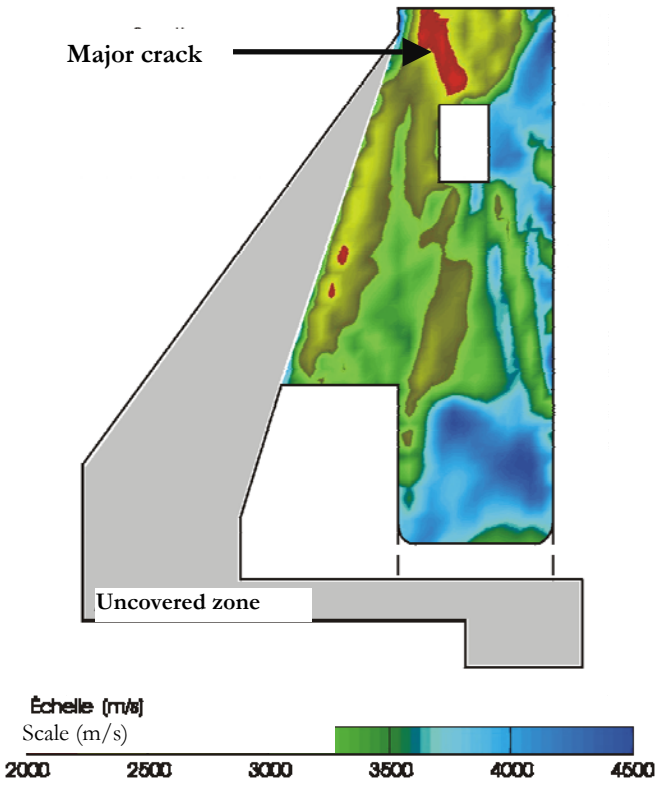

Figure 2: *P*-waves velocity tomography. Good condition concrete is associated with high-velocity areas.

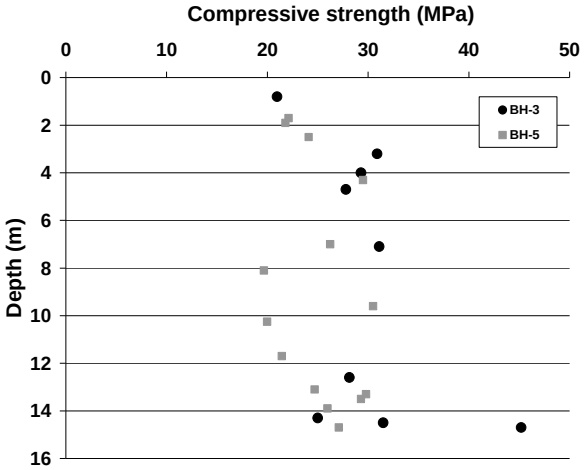

Figure 3: Compressive strength vs depth.

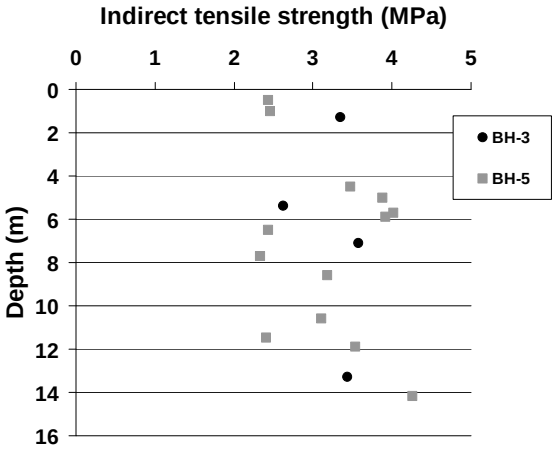

Figure 4: Indirect tensile strength vs depth.

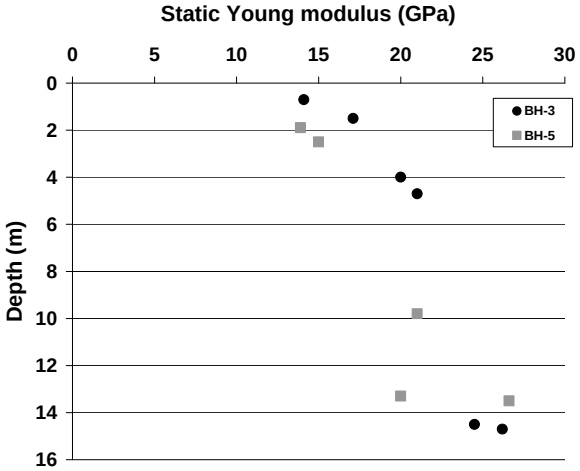

Figure 5: Static Young modulus vs depth.

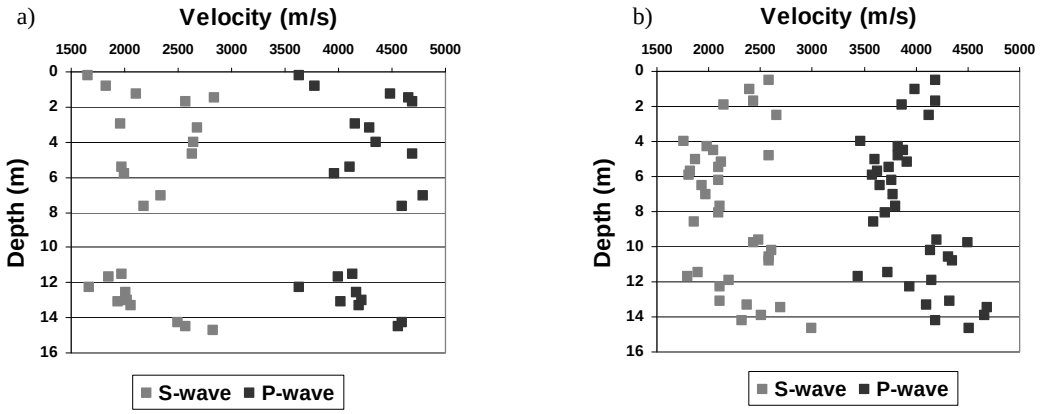

Figure 6 : Variation of *P*-wave and *S*-wave velocities in borehole a) BH-3, b) BH-5.

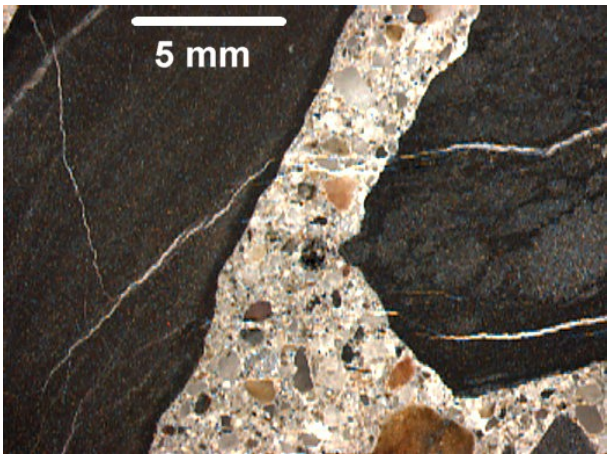

Figure 7: Various petrographic features typical of ASR: cracks filled with gel, extending into cement paste and connecting aggregates particles. Darker reaction rim is visible at the periphery of the left limestone particle.

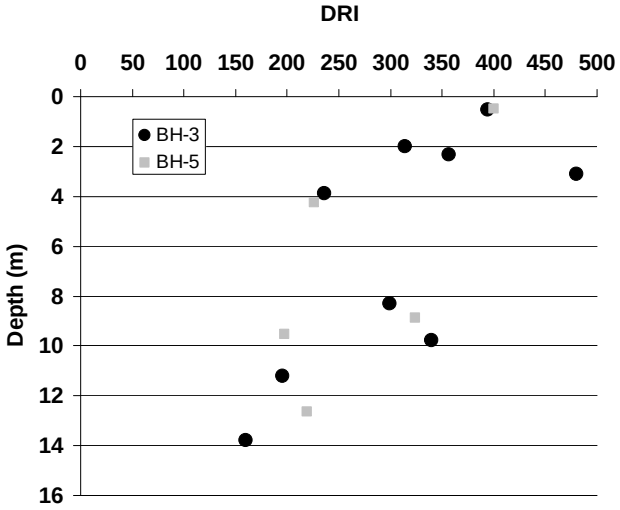

Figure 8: Results from the petrographic examination (*Damage Rating Index*).